



# Broken $^{206}\text{Pb}/^{238}\text{U}$ carbonate chronometers and $^{207}\text{Pb}/^{235}\text{U}$ fixes

Pieter Vermeesch<sup>1</sup>, Noah McLean<sup>2</sup>, Anton Vaks<sup>3</sup>, Tzahi Golan<sup>3</sup>, Sebastian F.M Breitenbach<sup>4</sup>, and Randall Parrish<sup>5</sup>

<sup>1</sup>University College London, London WC1E 6BT, United Kingdom

<sup>2</sup>University of Kansas, Lawrence, KS 66045, United States

<sup>3</sup>Geological Survey of Israel, 9692100 Jerusalem, Israel

<sup>4</sup>Northumbria University, Newcastle upon Tyne NE1 8ST, United Kingdom

<sup>5</sup>University of Portsmouth, Portsmouth PO1 3QL, United Kingdom

**Correspondence:** Pieter Vermeesch (p.vermeesch@ucl.ac.uk)

**Abstract.** Carbonate U–Pb dating has become a key tool for Quaternary palaeoclimatology and palaeoanthropology beyond the  $\sim 800$  ka age limit of Th–U disequilibrium dating. U–Pb geochronology is based on the paired radioactive decay of  $^{238}\text{U}$  to  $^{206}\text{Pb}$  and of  $^{235}\text{U}$  to  $^{207}\text{Pb}$ . Current carbonate U–Pb data processing algorithms rely mostly on the  $^{206}\text{Pb}/^{238}\text{U}$  clock and attach little weight to the  $^{207}\text{Pb}/^{235}\text{U}$  data. A key weakness of this approach is the need to correct the  $^{206}\text{Pb}/^{238}\text{U}$  data for initial  $^{234}\text{U}/^{238}\text{U}$  disequilibrium, which may cause an excess (or deficit) in radiogenic  $^{206}\text{Pb}$  compared to secular equilibrium. We introduce a new disequilibrium correction algorithm, using matrix exponentials. This algorithm can be used to undo the effects of U-series disequilibrium using either an assumed initial composition, or a measured set of modern  $^{234}\text{U}/^{238}\text{U}$  (and optionally  $^{230}\text{Th}/^{238}\text{U}$ ) activity ratios. Using a deterministic Bayesian inversion algorithm, we show that disequilibrium corrections work well for relatively young samples but become unreliable beyond 1.5 Ma and impossible beyond 2 Ma. Using theoretical models and real world examples from Siberia, South Africa and Israel, we show that the uncertainty of the disequilibrium correction of such old samples exceeds the correction itself. Previous ‘Monte Carlo’ error propagation methods underestimate these uncertainties by up to an order of magnitude. We advocate the use of the  $^{207}\text{Pb}/^{235}\text{U}$  isochron method as a more accurate and precise alternative to  $^{206}\text{Pb}/^{238}\text{U}$  geochronology for  $> 2$  Ma carbonates that are suspected to have experienced significant levels of initial  $^{234}\text{U}/^{238}\text{U}$  disequilibrium.

## 1 Introduction

Carbonate rocks are only a minor component of the continental crust. However, their scientific importance far outweighs their volumetric abundance. Biogenic carbonates and speleothems document the history of life, and of Earth’s climate and environment. For these carbonate archives to provide detailed time series of past changes requires an accurate and precise chronological framework, which are pinned down in absolute time with radiometric dating methods. Two techniques are commonly used for this purpose.  $^{230}\text{Th}/\text{U}$  dating is the method of choice for young ( $< 800$  ka; Cheng et al., 2013) samples whose  $^{230}\text{Th}$ ,  $^{234}\text{U}$  and  $^{238}\text{U}$  activities are out of secular equilibrium (Kaufman and Broecker, 1965; Ludwig, 2003b).  $^{206}\text{Pb}/^{238}\text{U}$  dating is the default method for older ( $> 800$  ka) rocks, in which the secular equilibrium between  $^{234}\text{U}$  and  $^{238}\text{U}$  has been restored (Richards et al., 1998; Woodhead et al., 2006; Roberts et al., 2020).



Ironically, the absence of detectable  $^{234}\text{U}/^{238}\text{U}$  disequilibrium compromises the accuracy of the  $^{206}\text{Pb}/^{238}\text{U}$  method. Any  
 25 initial excess or deficit of  $^{234}\text{U}$  and  $^{230}\text{Th}$  affects the  $^{206}\text{Pb}/^{238}\text{U}$  ratio and, hence, the age estimate derived therefrom. In clean,  
 detritus-free carbonates, it is often safe to assume the absence of initial  $^{230}\text{Th}$ . Unfortunately, this assumption is not valid  
 for  $^{234}\text{U}$ , which can be enriched (or occasionally depleted) relative to  $^{238}\text{U}$  by physiochemical processes such as (1)  $\alpha$ -recoil  
 ejection and preferential leaching of  $^{234}\text{U}$  from  $\alpha$ -damaged mineral sites, and (2) chemical fractionation between preferentially  
 oxidised  $^{234}\text{U}^{6+}$  and  $^{238}\text{U}^{4+}$  (Fleischer, 1982; Porcelli and Swarzenski, 2003). Corrections for initial  $^{234}\text{U}/^{238}\text{U}$  disequilibrium  
 30 can be done by either assuming a specific initial  $^{234}\text{U}/^{238}\text{U}$  activity ratio, or by inferring the initial ratio from any measured  
 residual  $^{234}\text{U}/^{238}\text{U}$ -disequilibrium. In Section 2 of this paper, we review the second approach using matrix exponentials.

Current disequilibrium correction algorithms use a ‘Monte Carlo’ approach to propagate the errors. In Section 3 we will  
 show that this approach can underestimate the analytical uncertainties of  $^{206}\text{Pb}/^{238}\text{U}$  dates by an order of magnitude and is  
 unreliable beyond  $\sim 2$  Ma. Unfortunately, this observation undermines the results of several published studies (Vermeesch  
 35 et al., 2025. A preprint of this accepted manuscript can be downloaded from <https://tinyurl.com/Taung2025>).

In Section 4 we introduce a deterministic Bayesian approach to estimate the uncertainties of disequilibrium-corrected  
 $^{206}\text{Pb}/^{238}\text{U}$  dates. We use this alternative algorithm to show that old, disequilibrium-corrected  $^{206}\text{Pb}/^{238}\text{U}$  dates are imprac-  
 tically imprecise, unless highly enriched initial  $^{234}\text{U}/^{238}\text{U}$  activity ratios can be ruled out *a priori*. The large uncertainty  
 associated with the  $^{206}\text{Pb}/^{238}\text{U}$  method degrades its ability to constrain reliable chronologies for  $> 2$  Ma carbonates. Fortu-  
 40 nately, we are able to present a more accurate approach. In Section 6 we make a case for the little used  $^{207}\text{Pb}/^{235}\text{U}$  clock as a  
 replacement for the  $^{206}\text{Pb}/^{238}\text{U}$  method.

$^{207}\text{Pb}/^{235}\text{U}$  isochrons are, essentially, immune to the effects of initial disequilibrium (apart from a minor correction for  
 $^{231}\text{Pa}$ , which becomes smaller with increasing age). In Section 7 we present examples from Siberia and Israel to show that  
 the  $^{207}\text{Pb}/^{235}\text{U}$  method is more accurate than the  $^{206}\text{Pb}/^{238}\text{U}$  method, whilst being less precise for young samples. Both the  
 45 Bayesian uncertainty estimation method and  $^{207}\text{Pb}/^{235}\text{U}$  isochrons have been implemented in the *IsoplotR* toolbox for  
 radiometric geochronology (Section 8).

This paper will use the following symbols and notations:

- $n_{38}, n_{34}, n_{30}, n_{26}$  and  $n_{06}$ : the number of atoms of  $^{238}\text{U}$ ,  $^{234}\text{U}$ ,  $^{230}\text{Th}$ ,  $^{226}\text{Ra}$  and  $^{206}\text{Pb}$ , respectively;
- $\lambda_{38}, \lambda_{35}, \lambda_{34}, \lambda_{32}, \lambda_{30}$  and  $\lambda_{26}$ : the radioactive decay constants of  $^{238}\text{U}$ ,  $^{235}\text{U}$ ,  $^{234}\text{U}$ ,  $^{232}\text{Th}$ ,  $^{230}\text{Th}$  and  $^{226}\text{Ra}$ , respec-  
 50 tively;
- $a_{xy}$ : the activity of  $xy$ . For example,  $a_{38} \equiv \lambda_{38}n_{38}$ ;
- $[34/38]_t$ : the present day  $^{234}\text{U}/^{238}\text{U}$  activity ratio (i.e.  $[a_{34}/a_{38}]$ );
- $[34/38]_i, [30/38]_i, [26/38]_i, [31/35]_i$ : the initial  $^{234}\text{U}/^{238}\text{U}$ ,  $^{230}\text{Th}/^{238}\text{U}$ ,  $^{226}\text{Ra}/^{238}\text{U}$  and  $^{231}\text{Pa}/^{235}\text{U}$  activity ratios,  
 respectively;



55 –  $[34/38]_m$  and  $s[34/38]_m$ : the measured  $^{234}\text{U}/^{238}\text{U}$  activity ratio and its standard error, respectively.

## 2 Disequilibrium corrections in a nutshell

Even though the U–Pb decay systems consist of numerous steps (14 for the  $^{238}\text{U} \rightarrow ^{206}\text{Pb}$  chain and 11 for the  $^{235}\text{U} \rightarrow ^{207}\text{Pb}$  chain), conventional U–Pb geochronology ignores this complexity and the method is mathematically treated as a set of simple parent-daughter pairs. This simplification is justified once a state of secular equilibrium is established between all the intermediate daughter products in the decay chains. Such secular equilibrium automatically emerges after 1 to 2 million years. As mentioned in Section 1, any disequilibrium that might exist prior to this secular equilibrium can be used as a chronometer in its own right.

Initial disequilibrium of the uranium decay series affects the accuracy of the U–Pb method. For example, ignoring any initial excess  $^{234}\text{U}$  results in an overestimated  $^{206}\text{Pb}/^{238}\text{U}$  age, and ignoring any initial  $^{231}\text{Pa}$  deficit results in an underestimated  $^{207}\text{Pb}/^{235}\text{U}$  age. Therefore, initial disequilibrium is one mechanism to produce discordant U–Pb results. In U–Pb geochronology of young (<5 Ma old) carbonates, the relative effect of initial disequilibrium can be very significant, and may potentially result in order-of-magnitude levels of bias. A disequilibrium correction is needed to remove this bias (Schärer, 1984; Engel et al., 2019).

If the intermediate daughter is sufficiently long lived and the sample is sufficiently young ( $t < 5/\lambda$ , say) to retain some of its disequilibrium, then the activity ratios can be back-calculated to the time of isotopic closure (assuming subsequent closed-system behaviour). This strategy applies to  $^{234}\text{U}/^{238}\text{U}$ -disequilibrium and, for very young samples, to  $^{230}\text{Th}/^{238}\text{U}$ -disequilibrium. The complex evolution of the decay series can be elegantly solved using matrix exponentials. For example, the  $^{238}\text{U} \rightarrow ^{206}\text{Pb}$  decay chain can be expressed in matrix form as follows:

$$\frac{\partial}{\partial t} \begin{bmatrix} n_{38} \\ n_{34} \\ n_{30} \\ n_{26} \\ n_{06} \end{bmatrix} = \begin{bmatrix} -\lambda_{38} & 0 & 0 & 0 & 0 \\ \lambda_{38} & -\lambda_{34} & 0 & 0 & 0 \\ 0 & \lambda_{34} & -\lambda_{30} & 0 & 0 \\ 0 & 0 & \lambda_{30} & -\lambda_{26} & 0 \\ 0 & 0 & 0 & \lambda_{26} & 0 \end{bmatrix} \begin{bmatrix} n_{38} \\ n_{34} \\ n_{30} \\ n_{26} \\ n_{06} \end{bmatrix} \quad (1)$$

75 The solution to Equation 1 is a so-called matrix exponential:

$$\begin{bmatrix} n_{38} \\ n_{34} \\ n_{30} \\ n_{26} \\ n_{06} \end{bmatrix} = \expm \left( \begin{bmatrix} -\lambda_{38} & 0 & 0 & 0 & 0 \\ \lambda_{38} & -\lambda_{34} & 0 & 0 & 0 \\ 0 & \lambda_{34} & -\lambda_{30} & 0 & 0 \\ 0 & 0 & \lambda_{30} & -\lambda_{26} & 0 \\ 0 & 0 & 0 & \lambda_{26} & 0 \end{bmatrix} t \right) \begin{bmatrix} n_{38} \\ n_{34} \\ n_{30} \\ n_{26} \\ n_{06} \end{bmatrix}_i \quad (2)$$

which expresses the present day amounts of the different isotopes as a function of the initial amounts. An interesting result is obtained by setting  $t = \infty$  in Equation 2 to estimate the activity ratio under secular equilibrium:



$$[34/38]_{\infty} = \frac{\lambda_{234}}{\lambda_{234} - \lambda_{238}} = 1.000055 \quad (3)$$

80 Note that this activity ratio is *not* exactly equal to unity. This is because 0.0055% of  $^{238}\text{U}$  is lost during  $^{234}\text{U}$ 's mean lifetime of  $1/\lambda_{34} = 354\text{ka}$ . Equation 2 can also be inverted to express the initial amounts as a function of the present day amounts:

$$\begin{bmatrix} n_{38} \\ n_{34} \\ n_{30} \\ n_{26} \\ n_{06} \end{bmatrix}_i = \expm \left( - \begin{bmatrix} -\lambda_{38} & 0 & 0 & 0 & 0 \\ \lambda_{38} & -\lambda_{34} & 0 & 0 & 0 \\ 0 & \lambda_{34} & -\lambda_{30} & 0 & 0 \\ 0 & 0 & \lambda_{30} & -\lambda_{26} & 0 \\ 0 & 0 & 0 & \lambda_{26} & 0 \end{bmatrix} t \right) \begin{bmatrix} n_{38} \\ n_{34} \\ n_{30} \\ n_{26} \\ n_{06} \end{bmatrix} \quad (4)$$

Equation 2 or 4 can be used to construct a concordia diagram in the presence of disequilibrium. If measured activity ratios are used to infer the initial conditions, then the concordia line terminates where those inferred activity ratios reach unrealistic values (e.g.,  $[34/38]_i = 500$  and  $[30/38]_i = 0$ ; Figure 1a). Beyond  $\sim 2\text{Ma}$ , it becomes very difficult to estimate  $[34/38]_i$  from  $[34/38]_m$ , and it is even more difficult to quantify the analytical uncertainty of the disequilibrium correction. In Section 3 we review the current approach to uncertainty estimation for initial disequilibrium correction and in Section 4 we propose an alternative approach, which offers significant advantages for samples that are close to secular equilibrium.

### 3 ‘Monte Carlo’ uncertainty estimation

90 Existing data processing software for disequilibrium-corrected  $^{206}\text{Pb}/^{238}\text{U}$  geochronology, such as `Isoplot` (Ludwig, 2003a) and `DQPB` (Pollard et al., 2023), estimate the uncertainty of the disequilibrium correction by Monte Carlo simulation. Given a linear array of isotopic data in Tera-Wasserburg space (i.e.  $^{207}\text{Pb}/^{206}\text{Pb}$  vs.  $^{238}\text{U}/^{206}\text{Pb}$ ), paired with an activity ratio measurement  $[34/38]_m$  with standard error  $s[34/38]_m$ , this approach works as follows:

1. Draw a random value  $[34/38]_t$  from a normal distribution with mean  $[34/38]_m$  and standard deviation  $s[34/38]_m$ .
- 95 2. Fit a straight line to the U–Pb data and find the  $[34/38]_i$ -value and isochron age ( $t$ ) that are consistent with both the U–Pb measurements and  $[34/38]_t$ . In other words, use Equation 4 to estimate  $[34/38]_i$  from  $[34/38]_t$ , and repeat this for different values of  $t$  until the linear fit to the U–Pb data is optimised.
3. Repeat steps 1 and 2 until the entire distribution of  $[34/38]_t$ -values has been sampled;
4. If step 2 fails, or produces physically impossible results (e.g.,  $t < 0$ ), then ignore the corresponding  $[34/38]_m$ -value.
- 100 Otherwise add the  $[34/38]_i$  and  $t$ -values to a list of acceptable results.
5. Use the spread of the acceptable  $[34/38]_i$  and  $t$ -values to quantify their respective uncertainties.



For the purpose of the present study, we have implemented our own version of this algorithm, using R and IsoplotR (Vermeesch, 2018). The only major difference between our code and Isoplot/DQPB is that it does not sample the  $[34/38]_m$ -distribution randomly, but uses a targeted approach to sample  $[34/38]_m$  as a sequence of regularly spaced normal quantiles. This is faster and produces deterministic results that do not depend on the seed of a random number generator. Figure 1 summarises the application of this approach using the ‘Corchia’ dataset of Pollard et al. (2023), producing identical results to Isoplot/DQPB. To reflect this equivalence of outcomes, we will refer to our version of the algorithm as a ‘Monte Carlo’ method, despite the fact that it does not actually use a random number generator.

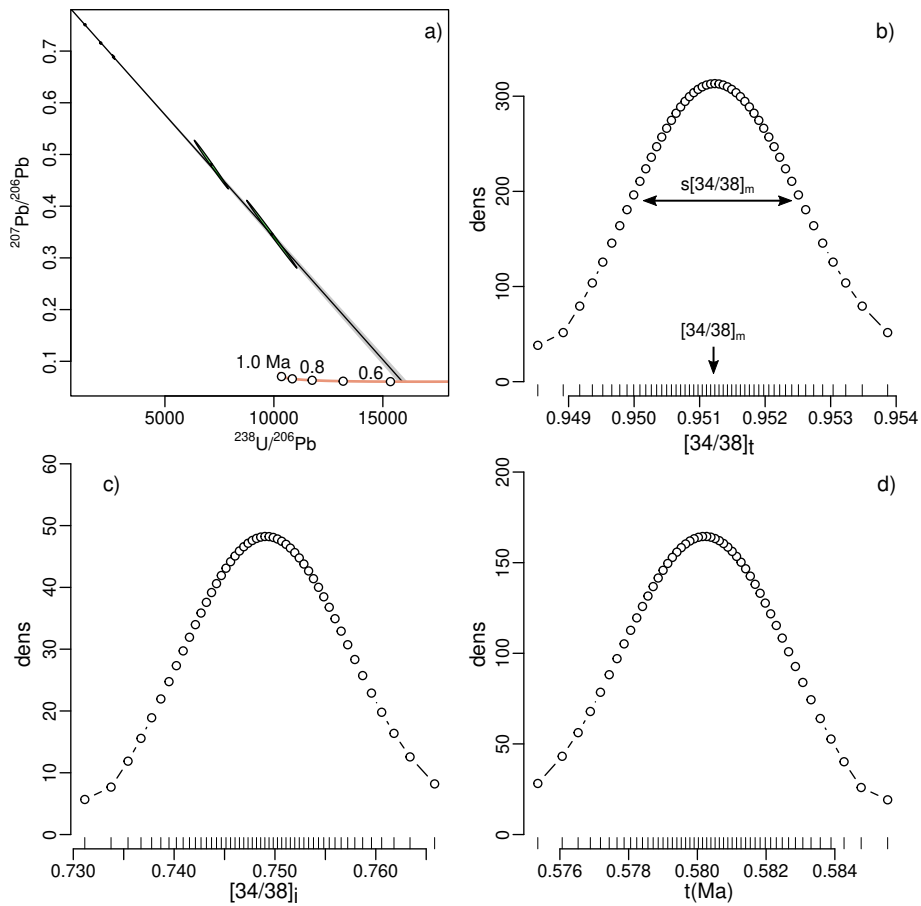


**Figure 1.** Output of the ‘Monte Carlo’ algorithm for the Corchia dataset of Pollard et al. (2023). a) Tera-Wasserburg concordia diagram with disequilibrium-corrected isochron ( $t = 0.5803$  Ma); b) 50 representative samples from the distribution of  $^{234}\text{U}/^{238}\text{U}$  activity ratio measurements; c) The corresponding initial  $^{234}\text{U}/^{238}\text{U}$  activity ratios; d) The isochron ages corresponding to the  $[34/38]_i$  values presented in panel c.

Next, let us apply the same approach to older samples, such as ‘Hoogland’ dataset of Pickering et al. (2019). The uncorrected U–Pb isochron age for this sample is 7.407 Ma, which is 30 half-lives of  $^{234}\text{U}$ . Consequently, the measured present-day  $^{234}\text{U}/^{238}\text{U}$  activity ratio is statistically indistinguishable from secular equilibrium, at  $[34/38]_m = 1.0016 \pm 0.001$  (1 SE). Despite the lack of measurable disequilibrium, the ‘Monte Carlo’ approach appears to have successfully applied a disequilibrium



correction, resulting in a corrected age that is less than half the uncorrected age, with a precision of better than 15% (Figure 2).  
 115 How is this possible? The answer lies in the rejected solutions (step 4 of the algorithm), which are marked in black in Figure 2b. Ignoring these ‘physically impossible’ initial ratios suppresses the equilibrium solutions and skews the distribution of Monte Carlo solutions towards high  $[34/38]_i$ -values (Figure 2c) and young ages (Figure 2d).

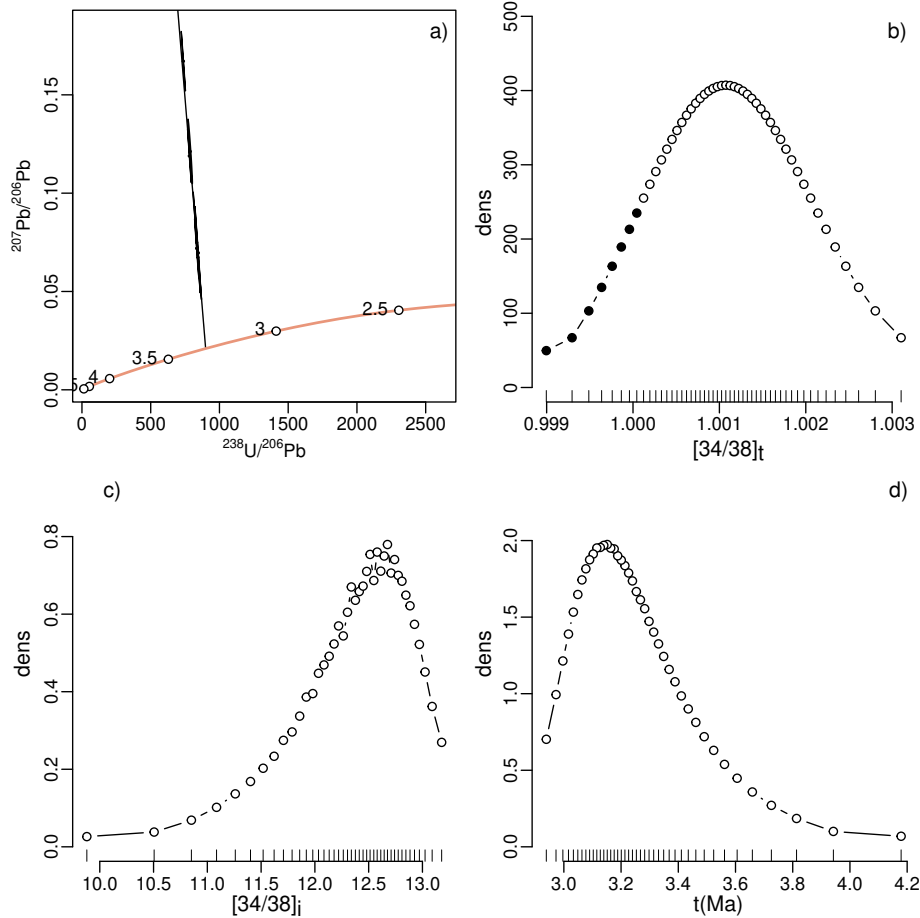


**Figure 2.** Output of the ‘Monte Carlo’ algorithm for the Hoogland dataset of Pickering et al. (2019). Panels a) – d) are as in Figure 1. The black dots in panel b) mark synthetic replicates that are rejected because they yield physically impossible  $[34/38]_i$  and/or  $t$ -values. The results shown in panels c and d are consistent with the published values.

To demonstrate that the result of Figure 2 is wrong, let us replace the measured  $^{234}\text{U}/^{238}\text{U}$  activity ratio with the equilibrium  
 120 ratio (Equation 3):

$$[34/38]_m = [34/38]_\infty \pm 0.001$$

Plugging this value into the ‘Monte Carlo’ algorithm yields an impossible result (Figure 3). It has applied a disequilibrium correction without any actual disequilibrium, by ignoring exactly half of the  $[34/38]_t$  distribution (Figure 3b). This was neces-

sary because, for this old sample, essentially any  $[34/38]_t$  value that is less than the equilibrium ratio would require a negative  
 125  $[34/38]_i$  ratio, or a negative isochron age  $t$ .

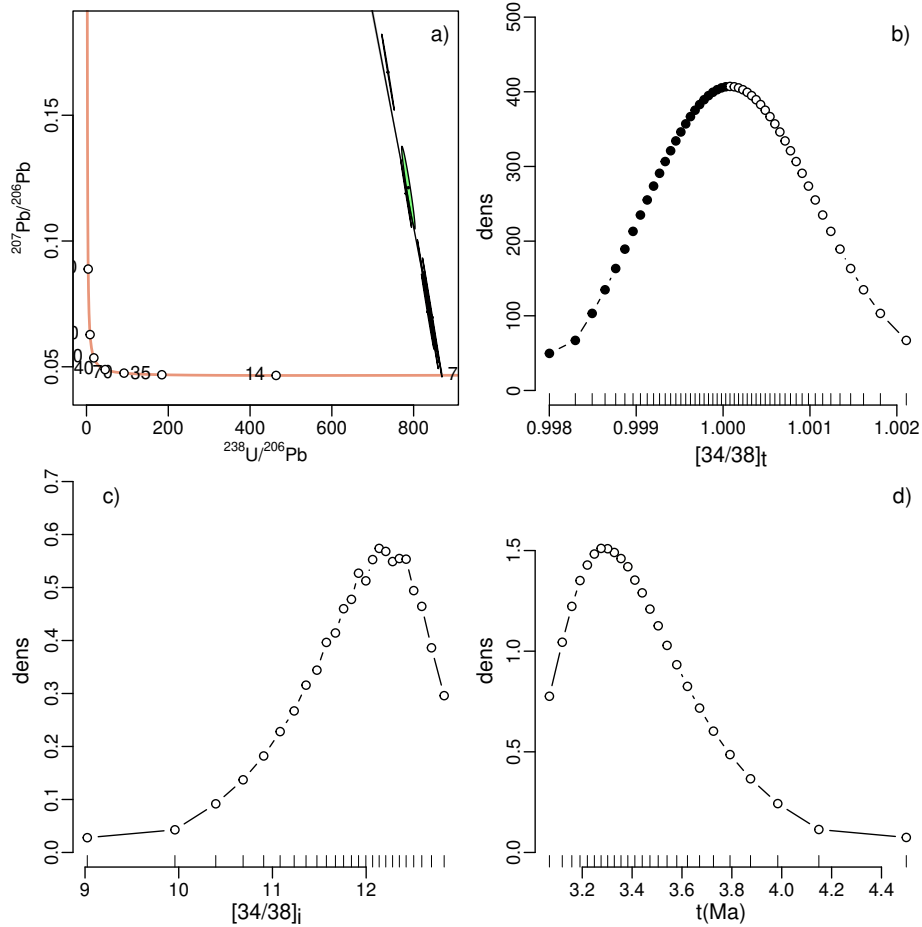


**Figure 3.** The same data as Figure 2, but replacing  $[34/38]_m$  with the equilibrium ratio. Note that half of the synthetic replicates have been rejected (black circles). Even though there is absolutely no evidence for disequilibrium, the ‘Monte Carlo’ produces a corrected isochron age (panel d) that is half the uncorrected value (panel a). This result is clearly wrong.

#### 4 A Bayesian approach

The previous section showed that the ‘Monte Carlo’ algorithm produces incorrect results for samples whose  $[34/38]_t$ -distributions fall within, say, three standard deviations (i.e.,  $3 \times s[34/38]_m$ ) from secular equilibrium. In this section we propose a Bayesian  
 130 algorithm that can be applied to any values of  $[34/38]_m$  and  $s[34/38]_m$ :

1. Define a prior distribution for  $[34/38]_i$ . Here we use a uniform distribution from  $m$  to  $M$  (e.g.,  $m = 0$  and  $M = 20$  for  $[34/38]_i$ -values running from 0 to 20). However, this could easily be replaced by a more informative prior.



2. Draw a random sample from this prior distribution, carry out a constrained isochron regression and register the resulting age ( $t$ ) and corresponding  $[34/38]_t$ -value. In other words, use Equation 2 to estimate  $[34/38]_t$  from  $[34/38]_i$ , and repeat this for different values of  $t$  until the linear fit to the U–Pb data is optimised. Register the (log)likelihood of this linear fit using the same algorithm as used for regular U–Pb isochron regression (Ludwig, 1998; Vermeesch, 2020).
3. Calculate the likelihood of the inferred  $[34/38]_t$ -values under a normal distribution with mean  $[34/38]_m$  and standard deviation  $s[34/38]_m$ . Combine with the likelihood of the linear fit (obtained in step 2) to produce the ‘posterior’ probability of initial ratios.
4. Repeat steps 2 and 3 to constrain the posterior distributions of  $[34/38]_i$  and  $t$ . This can either be done using a Markov chain, or with a targeted approach of appropriately spaced  $[34/38]_i$  values.

Applying this method to the 580 ka Corchia example (Figure 4) yields essentially identical results to the ‘Monte Carlo’ algorithm (Figure 1).

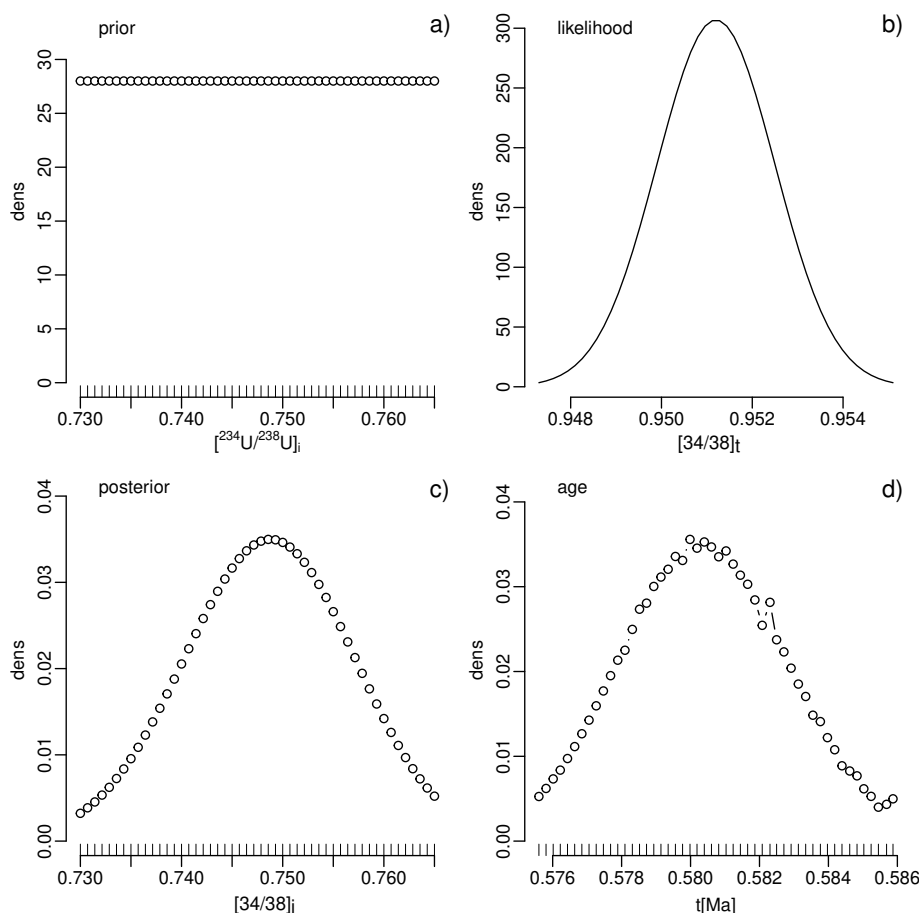


**Figure 4.** The same data as Figure 1, but using the Bayesian approach. For this relatively young sample, the Bayesian method yields similar results to the ‘Monte Carlo’ solution.





145 However, when the Bayesian approach is applied to the older Hoogland data (Figure 5), it produces a very different result than the ‘Monte Carlo’ approach (Figure 2). The posterior distributions for the Hoogland data (shown in Figure 5c and d) still have maxima at  $[34/38]_i = 12$  and  $t = 3.3$  Ma, just like the ‘Monte Carlo’ distributions (Figures 2c and d). But unlike the ‘Monte Carlo’ solution, the result of the Bayesian approach also assigns a significant likelihood to older ages, including the uncorrected age of 7.4 Ma (and older). The similarity of this posterior distribution to the prior distribution reflects the fact that

150 the measured  $^{234}\text{U}/^{238}\text{U}$  activity ratio contains relatively little information. The resulting uncertainties are huge, but correctly reflect our ignorance about the true extent of the disequilibrium in this case (Vermeesch et al., 2025). A preprint of this accepted manuscript can be downloaded from <https://tinyurl.com/Taung2025>.

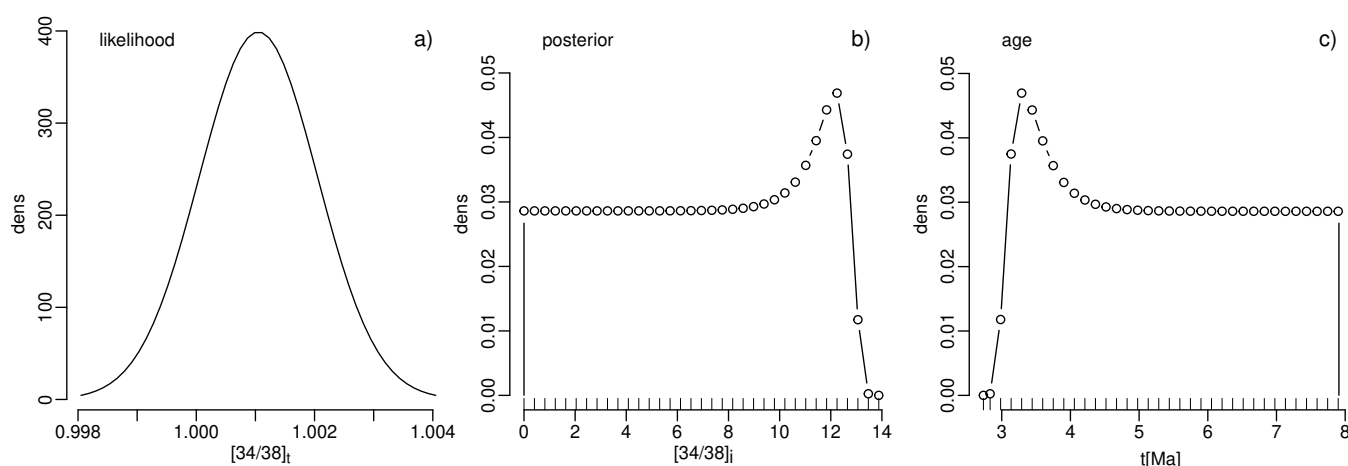


**Figure 5.** Application of the Bayesian approach to the Hoogland data of Pickering et al. (2019). A uniform prior was used but is not shown. The mode of the posterior distribution agrees with the mode of the ‘Monte Carlo’ solution of Figure 2. However, whereas the ‘Monte Carlo’ algorithm suggests a high degree of confidence in the disequilibrium correction, the Bayesian approach shows that one cannot rule out a much higher age of the sample. In fact, the uncorrected  $^{206}\text{Pb}/^{206}\text{U}$  age of 7.4 Ma is almost as likely as the corrected age of 3.3 Ma.

Finally, changing the  $[34/38]_m$ -ratio to the equilibrium value (Figure 6) produces a posterior distribution that is nearly

155 identical to the prior distribution. This means that the likelihood function contains almost no information. In other words: the measured  $^{234}\text{U}/^{238}\text{U}$  activity ratio does not tell us anything about the initial disequilibrium (except that  $[34/38]_i < 12$ ). If we truly believe that the sample may have experienced extreme  $^{234}\text{U}/^{238}\text{U}$  disequilibrium, then it is not possible to undo the effects of this disequilibrium using the modern (measured)  $^{234}\text{U}/^{238}\text{U}$  activity ratio.

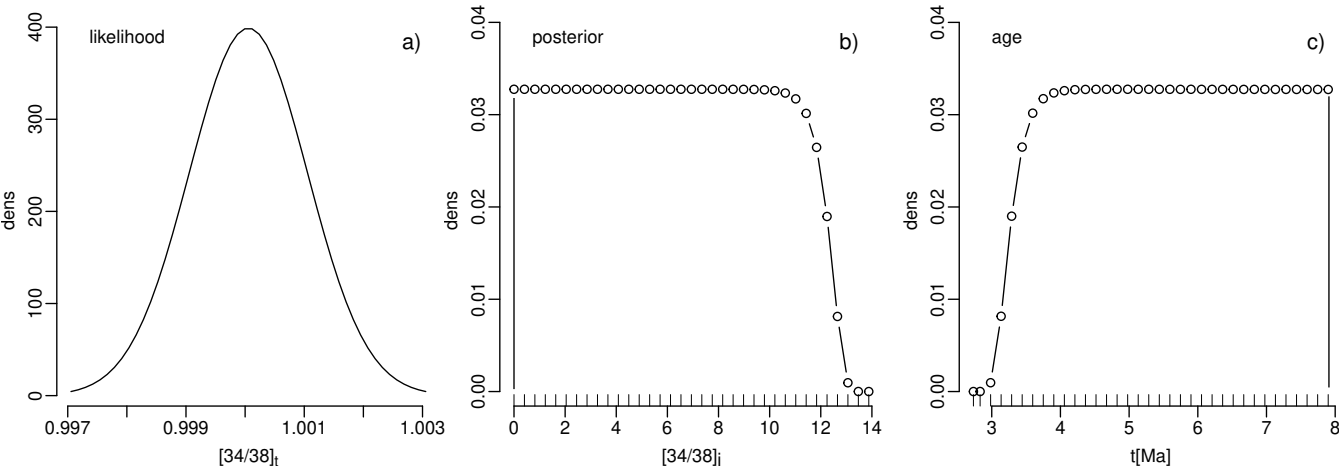


**Figure 6.** Bayesian alternative to the modified Hoogland example of Figure 3. The posterior distribution is very similar to the uniform prior (for  $[34/38]_i < 12$ ). This reflects the fact that the likelihood function (panel a) contains almost no information, because it is centred around the equilibrium ratio. The only conclusion that can be drawn from this dataset is that  $3 < t < 8$  Ma.

160 **5 The case against  $^{206}\text{Pb}/^{238}\text{U}$ -dating of  $> 2$  Ma carbonates**

To summarise the conclusions of Sections 3 and 4, disequilibrium corrections using measured  $^{234}\text{U}/^{238}\text{U}$  activity ratios are only feasible if those activity ratios are statistically distinguishable from secular equilibrium. To turn these conclusions into quantitative guidelines, let us assume that  $^{234}\text{U}/^{238}\text{U}$ -activity ratios can be measured with a precision of 0.2% (i.e.  $s[34/38]_m/[34/38]_m = 0.002$ ), and define “statistically distinguishable” as “at least  $3 \times s[34/38]_m$  removed from secular equilibrium”. Under these assumptions, a sample with  $[34/38]_i < 2.7$  would become indistinguishable from secular equilibrium after 2 Ma. In other words, it is impossible to correct a 2 Ma sample whose  $[34/38]_i = 2.7$ , say. The uncorrected  $^{206}\text{Pb}/^{238}\text{U}$  isochron age of such a sample would be 2.60 Ma, corresponding to a bias of 30%. Table 1 shows the outcomes of the same exercise for a range of other ages.

**Table 1.** Sensitivity test of the  $^{206}\text{Pb}/^{238}\text{U}$  method using selected ages.

| true age (Ma)                  | 0.5  | 1    | 1.5  | 2    | 2.5  | 3.0  |
|--------------------------------|------|------|------|------|------|------|
| minimum resolvable $[34/38]_i$ | 1.02 | 1.10 | 1.41 | 2.70 | 7.95 | 29.5 |
| maximum bias (%)               | 1.1  | 3.3  | 9.6  | 30   | 98   | 336  |

170 Based on these calculations, we judge the  $^{206}\text{Pb}/^{238}\text{U}$  method to be unreliable beyond 1.5 Ma, and impossible beyond 2 Ma unless initial  $^{234}\text{U}/^{238}\text{U}$  disequilibrium can be confidently ruled out. Thankfully, there is a solution to the conundrum of  $^{234}\text{U}/^{238}\text{U}$ -disequilibrium. This solution is the  $^{207}\text{Pb}/^{235}\text{U}$  isochron method (Richards et al., 1998; Engel et al., 2019; Vaks et al., 2020; Vermeesch et al., 2025. A preprint of this accepted manuscript can be downloaded from <https://tinyurl.com/Taung2025>).



## 175 6 A $^{207}\text{Pb}/^{235}\text{U}$ fix to $^{206}\text{Pb}/^{238}\text{U}$ 's problems

In the previous section, we showed that the accuracy of the  $^{206}\text{Pb}/^{238}\text{U}$  method is undermined by the extreme  $^{234}\text{U}$ -enrichment that is observed in some groundwaters (e.g., Kronfeld et al., 1994). This problem can be solved by avoiding  $^{234}\text{U}$  altogether and sidestepping the  $^{238}\text{U}$ - $^{206}\text{Pb}$  decay chain in favour of the  $^{235}\text{U}$ - $^{207}\text{Pb}$  decay chain.

180 There are two kinds of  $^{207}\text{Pb}/^{235}\text{U}$ -isochron. The simplest kind plots  $^{204}\text{Pb}/^{207}\text{Pb}$ -ratios against  $^{204}\text{Pb}/^{235}\text{U}$ -ratios, defining the following linear relationship:

$$\left[ \frac{^{204}\text{Pb}}{^{207}\text{Pb}} \right] = \left[ \frac{^{204}\text{Pb}}{^{207}\text{Pb}} \right]_i \left\{ 1 - \left[ \frac{^{235}\text{U}}{^{207}\text{Pb}} \right] (\exp[\lambda_{35}t] - 1) \right\} \quad (5)$$

where  $^{204}\text{Pb}$  is used as a proxy for common Pb. Alternatively, one can also use  $^{208}\text{Pb}$  to fulfil this role. This gives rise to a  $^{208}\text{Pb}_i/^{207}\text{Pb}$  vs.  $^{235}\text{U}/^{207}\text{Pb}$  isochron, where  $^{208}\text{Pb}_i$  is the non-radiogenic  $^{208}\text{Pb}$ -component (with the decay products of  $^{232}\text{Th}$  removed). Equation 5 is then replaced with:

$$185 \left[ \frac{^{208}\text{Pb}_i}{^{207}\text{Pb}} \right] = \left[ \frac{^{208}\text{Pb}}{^{207}\text{Pb}} \right]_i \left\{ 1 - \left[ \frac{^{235}\text{U}}{^{207}\text{Pb}} \right] (\exp[\lambda_{35}t] - 1) \right\} \quad (6)$$

where

$$\left[ \frac{^{208}\text{Pb}_i}{^{207}\text{Pb}} \right] = \left[ \frac{^{208}\text{Pb}}{^{207}\text{Pb}} \right] - \left[ \frac{^{232}\text{Th}}{^{207}\text{Pb}} \right] \exp[\lambda_{32}t] + 1 \quad (7)$$

in which the  $^{232}\text{Th}/^{207}\text{Pb}$ -ratio can be obtained from the product of the  $^{232}\text{Th}/^{238}\text{U}$ ,  $^{238}\text{U}/^{235}\text{U}$  and  $^{235}\text{Th}/^{207}\text{Pb}$  ratios. Because  $^{232}\text{Th}$  is insoluble in water, radiogenic  $^{208}\text{Pb}$  is often absent from carbonates. Therefore, it is generally safe to assume that  
 190  $[^{208}\text{Pb}_i/^{207}\text{Pb}] \approx [^{208}\text{Pb}/^{207}\text{Pb}]$ .

Unlike the  $^{238}\text{U} \rightarrow ^{206}\text{Pb}$  decay system, the  $^{235}\text{U} \rightarrow ^{207}\text{Pb}$  decay chain does not include  $^{234}\text{U}$  or  $^{230}\text{Th}$ . It therefore does not require correction for initial disequilibrium of those nuclides. Of course, this does not mean that the  $^{235}\text{U} \rightarrow ^{207}\text{Pb}$  method is entirely free of disequilibrium issues. There is one intermediate daughter,  $^{231}\text{Pa}$ , which requires a correction. Due to  $^{231}\text{Pa}$ 's short half-life of 32.65 kyr, it is generally not possible to measure any remaining disequilibrium. Therefore, the  $[31/35]_i$ -value  
 195 must be assumed.

Fortunately, Pa is chemically similar to Th, being insoluble in water. Therefore,  $^{231}\text{Pa}$  is always depleted relative to  $^{235}\text{U}$  in carbonates. So whereas  $[34/38]_i$  can vary anywhere between 0 and 12 (Kronfeld et al., 1994),  $[31/35]_i$  is always less than 1 and can be safely assumed to be zero. In a worst case scenario, in which one assumes  $[31/35]_i = 0$  but the true activity ratio is  $[31/35]_i = 1$ , this would only bias the  $^{235}\text{Pb}/^{235}\text{U}$  age by a relatively small amount (Table 2).

**Table 2.** Sensitivity test of the  $^{207}\text{Pb}/^{235}\text{U}$  method against  $^{231}\text{Pa}$  disequilibrium.

|     |                  |     |     |     |     |     |     |
|-----|------------------|-----|-----|-----|-----|-----|-----|
| 200 | true age (Ma)    | 0.5 | 1   | 1.5 | 2   | 2.5 | 3.0 |
|     | maximum bias (%) | 10  | 4.9 | 3.2 | 2.4 | 1.9 | 1.6 |



The degree of potential bias of the  $^{207}\text{Pb}/^{235}\text{U}$  method decreases with increasing age, unlike the  $^{206}\text{Pb}/^{238}\text{U}$  method, whose bias increases with age (Table 1). In this sense, the  $^{207}\text{Pb}/^{235}\text{U}$  and  $^{206}\text{Pb}/^{238}\text{U}$  methods are complementary to each other. The  $^{207}\text{Pb}/^{235}\text{U}$  is most accurate for samples older than 1 Ma, whereas the  $^{206}\text{Pb}/^{238}\text{U}$  is more accurate for samples younger than 1 Ma. Note that the latter is similar to the applicability range of the  $^{230}\text{Th}/\text{U}$  method. So one could argue that the  $^{206}\text{Pb}/^{238}\text{U}$  method is of limited use to carbonate U–Pb geochronology (except to infer  $[34/38]_i$ ; Engel et al., 2019). Although the  $^{207}\text{Pb}/^{235}\text{U}$  method outperforms the  $^{206}\text{Pb}/^{238}\text{U}$  method at 1 Ma in terms of accuracy, its poorer precision means that its potential benefits do not materialise until 2 Ma. In the next Section, we will demonstrate this by applying both methods to three different case studies.

## 7 Case studies

Having made a largely theoretical case against  $^{206}\text{Pb}/^{238}\text{U}$  dating and for  $^{207}\text{Pb}/^{235}\text{U}$  dating of old ( $> 2$  Ma) carbonates that are suspected to have experienced initial  $^{234}\text{U}/^{238}\text{U}$  disequilibrium, we will now compare and contrast the two chronometers using three practical case studies. The first example will demonstrate the accuracy of the  $^{207}\text{Pb}/^{235}\text{U}$  method by showing its consistency with disequilibrium-corrected  $^{206}\text{Pb}/^{238}\text{U}$  dates of young ( $< 2$  Ma) samples. The second example will use ID-TIMS data to show that the  $^{207}\text{Pb}/^{235}\text{U}$  method produces more accurate, more consistent, and more precise results than the  $^{206}\text{Pb}/^{238}\text{U}$  method for older ( $> 2$  Ma) carbonates. In the third case study we apply the  $^{207}\text{Pb}/^{235}\text{U}$  method to LA-ICP-MS data using  $^{208}\text{Pb}$  as a proxy for common Pb. In addition to highlighting a successful application where the  $^{207}\text{Pb}/^{235}\text{U}$  method produces demonstrably superior results to the  $^{206}\text{Pb}/^{238}\text{U}$  method, this dataset also illustrates limitations of the  $^{207}\text{Pb}/^{235}\text{U}$  approach with a sample that yields a precise  $^{206}\text{Pb}/^{238}\text{U}$  isochron and an unusably imprecise  $^{207}\text{Pb}/^{235}\text{U}$  isochron.

### 7.1 ID-ICP-MS data from Siberia

A rich dataset of 72 speleothem dates is available from Ledyanaya Lenskaya (LLC) and Botovskaya caves in Siberia (Vaks et al., 2020). These authors used the U–Pb method to extend an important palaeoclimatological archive that was previously dated using the  $^{230}\text{Th}$ – $^{234}\text{U}$ – $^{238}\text{U}$  disequilibrium method (Vaks et al., 2013a). Samples were analysed by isotope dilution ICP-MS and were found to exhibit a significant level of  $^{234}\text{U}/^{238}\text{U}$  disequilibrium. U–Pb ages were estimated using a two-step procedure. First, the common-Pb contribution was removed by two-point isochron regression through an inherited composition that was inferred by inspection of apparent linear trends in Tera-Wasserburg concordia space. Second, a  $^{234}\text{U}/^{238}\text{U}$  disequilibrium correction was applied to the radiogenic end-member composition, using the procedures described in Section 2. This correction combined the measured  $^{234}\text{U}/^{238}\text{U}$  activity ratios with an assumed absence of initial  $^{230}\text{Th}$  and  $^{231}\text{Pa}$ .

The inferred  $[34/38]_i$ -values were  $\sim 2$  and 3–5 for LLC and Botovskaya cave, respectively. This corresponds to an age correction of 15% for LLC and 60% for Botovskaya (Figure 7). Uncertainties were estimated using the Bayesian procedure of Section 4, making the optimistic assumption that the analytical uncertainty of the  $[34/38]_m$ -measurements faithfully captures all sources of dispersion. The scatter of the  $[34/38]_i$ -values suggests that this may not be the case. This caveat notwithstanding,

the disequilibrium-corrected  $^{206}\text{Pb}/^{238}\text{U}$  and  $^{207}\text{Pb}/^{235}\text{U}$  ages are in excellent agreement, overlapping within uncertainty in all but four of the samples.

The  $^{207}\text{Pb}/^{235}\text{U}$  age uncertainty is invariably larger than the  $^{206}\text{Pb}/^{238}\text{U}$  age uncertainty. In fact, below  $\sim 1$  Ma, it could be argued that the  $^{207}\text{Pb}/^{235}\text{U}$  age uncertainties are unusably imprecise ( $s[t]/t > 50\%$ ). However, above 1 Ma, the uncertainty reduces to acceptable levels ( $s[t]/t < 5\%$ ). Extrapolating this trend further into the past confirms the earlier assertion that beyond 2 Ma, the  $^{207}\text{Pb}/^{235}\text{U}$  method outperforms the  $^{206}\text{Pb}/^{238}\text{U}$  method in both accuracy and precision (Vermeesch et al., 2025). A preprint of this accepted manuscript can be downloaded from <https://tinyurl.com/Taung2025>.

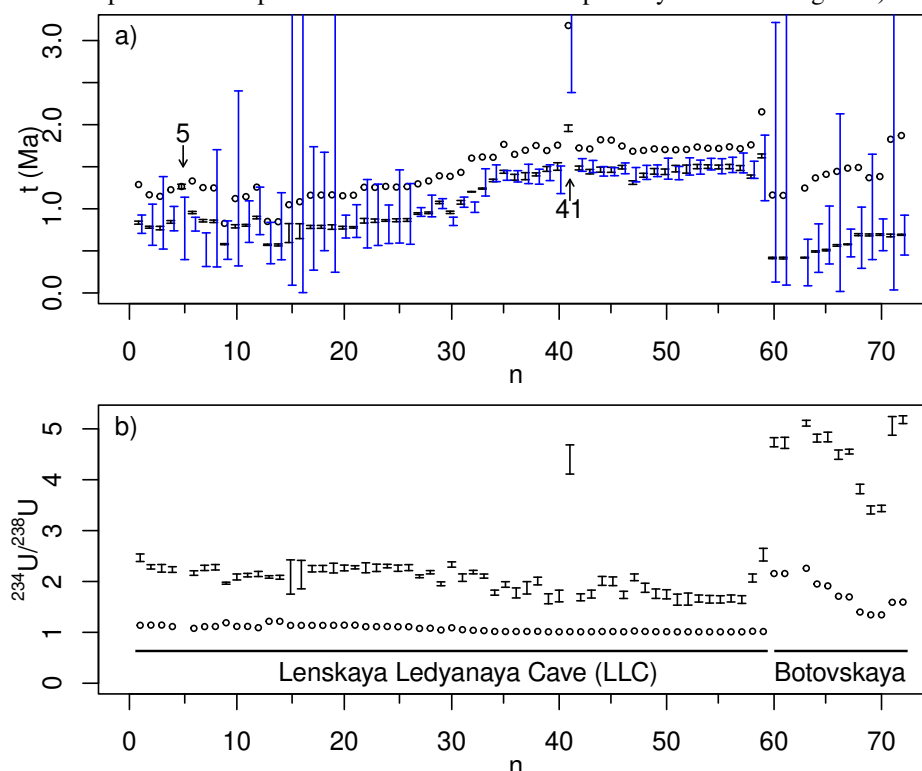


**Figure 7.** Reanalysis of the speleothem data of Vaks et al. (2020). a) uncorrected (circles) and corrected (black error bars)  $^{206}\text{Pb}/^{238}\text{U}$  dates, juxtaposed next to the  $^{207}\text{Pb}/^{235}\text{U}$  dates (blue error bars) for the same samples. b) measured ( $[34/38]_m$ , circles) and inferred initial ( $[34/38]_i$ , error bars)  $^{234}\text{U}/^{238}\text{U}$ -activity ratios. All error bars represent Bayesian 95% credible intervals. Sample 5 does not have a  $[34/38]_m$  measurement and was assumed to be in secular equilibrium. Sample 41 is an outlier that has an anomalously high common Pb concentration and is only included for the sake of completeness.

## 7.2 ID-TIMS data for ASH-15

ASH-15 is a carbonate U–Pb dating reference material sourced from a flowstone in Ashalim cave of southern Israel (Nuriel et al., 2021). 37 ID-TIMS measurements were obtained from the flowstone, including 12 from horizon D and 25 from horizon



K. The latter are shown in Figure 8. Nuriel et al. (2021) report an uncorrected semitotal-Pb/U isochron age of  $2.965 \pm 0.011$  Ma for ASH-15.

245 No  $^{234}\text{U}/^{238}\text{U}$  activity ratio measurements are available for ASH-15D and ASH-15K. However, two other horizons of the same flowstone (ASH-15A+B and ASH-15C1) are characterised by  $[34/38]_m$ -values of  $0.99939 \pm 0.00108$  and  $0.99925 \pm 0.0015$ , indistinguishable from secular equilibrium. Younger flowstones in the the Ashelim cave yield an average  $[34/38]_i$ -value of 1.0470 with a standard deviation of 0.01492 (Vaks et al., 2010, 2013b). Despite this lack of observable disequilibrium, Mason et al. (2013) suggest a  $[34/38]_i$ -value of 1.5–2.0 to explain the minor degree of discordance of the common-Pb corrected  
 250 Tera-Wasserburg ratios.

To investigate the effect of initial U-series disequilibrium on ASH-15, Figures 8a and b apply the Bayesian inversion algorithm to the ASH-15K data, using the  $[34/38]_m$ -value of ASH-15D and assuming that  $[30/38]_i = 0$  (i.e. no initial  $^{230}\text{Th}$ ). The posterior distribution for  $[34/38]_i$  is shifted towards low activity ratios, with a mode at  $[34/38]_m = 0.29$  (Figure 8a). As expected, initial equilibrium is very plausible ( $P([34/38]_i > 1.0) = 0.40$ ). The initial activity ratio preferred by Mason et al.  
 255 (2013) cannot be ruled out either, but is less likely ( $P([34/38]_i > 1.5) = 0.17$ ,  $P([34/38]_i > 2.0) = 0.03$ ).

The posterior distribution of the  $^{206}\text{Pb}/^{238}\text{U}$  isochron age spans a 10% range, from 2.5 to 3.3 Ma, with a mode at 3.23 Ma (Figure 8b). This range includes the following end-member scenarios (Figure 8c):

1. An uncorrected  $^{206}\text{Pb}/^{238}\text{U}$  isochron age of  $3.024 \pm 0.074$  Ma, assuming  $[34/38]_i = [30/38]_i \approx 1$ .
2. A corrected  $^{206}\text{Pb}/^{238}\text{U}$  isochron age of  $3.133 \pm 0.074$  Ma, assuming  $[34/38]_i \approx 1$  and  $[30/38]_i = 0$ .
- 260 3. A corrected  $^{206}\text{Pb}/^{238}\text{U}$  isochron age of  $2.779 \pm 0.074$  Ma, assuming  $[34/38]_i = 2.0$  and  $[30/38]_i = 0$ .

In contrast with the widely varying scenarios for the  $^{206}\text{Pb}/^{238}\text{U}$  method, the  $^{207}\text{Pb}/^{235}\text{U}$  isochron age calculation is straightforward:

1. An uncorrected  $^{207}\text{Pb}/^{235}\text{U}$  isochron age of  $3.039 \pm 0.068$  Ma, assuming  $[31/35]_i \approx 1$ .
2. A corrected  $^{207}\text{Pb}/^{235}\text{U}$  isochron age of  $3.086 \pm 0.068$  Ma, assuming  $[31/35]_i = 0$ .

265 which are nearly identical. The near perfect agreement between the second scenario of the  $^{206}\text{Pb}/^{238}\text{U}$  age and the  $^{207}\text{Pb}/^{235}\text{U}$  isochron age suggests that ASH-15 did not experience any significant initial  $^{234}\text{U}/^{238}\text{U}$ -disequilibrium. This inference fits well with all the other flowstones in the Ashelim cave (Vaks et al., 2010, 2013b).

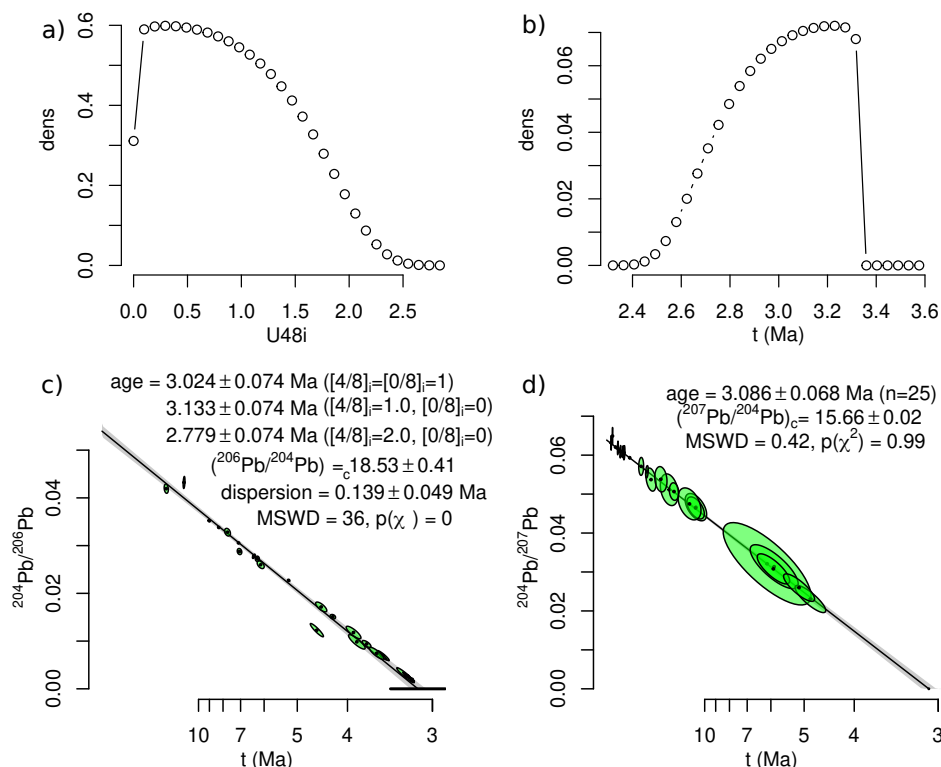


**Figure 8.** ID-TIMS U–Pb data for flowstone ASH-15K (Nuriel et al., 2021). a) posterior distribution for the initial  $^{234}\text{U}/^{238}\text{U}$  activity ratio; b) posterior distribution for the disequilibrium-corrected  $^{206}\text{Pb}/^{238}\text{U}$  isochron age, based on the  $[34/38]_m$ -measurement of Vaks et al. (2010); c) the  $^{206}\text{Pb}/^{238}\text{U}$  isochron, fitted using the model-3 algorithm of Vermeesch (2024), with the excess dispersion shown as a horizontal 95% error bar; and d) the model-1  $^{207}\text{Pb}/^{235}\text{U}$  isochron. The grey uncertainty bands represent the standard errors of the isochron fits and do not reflect the Bayesian credible intervals.

### 7.3 LA-ICP-MS data from Siberia

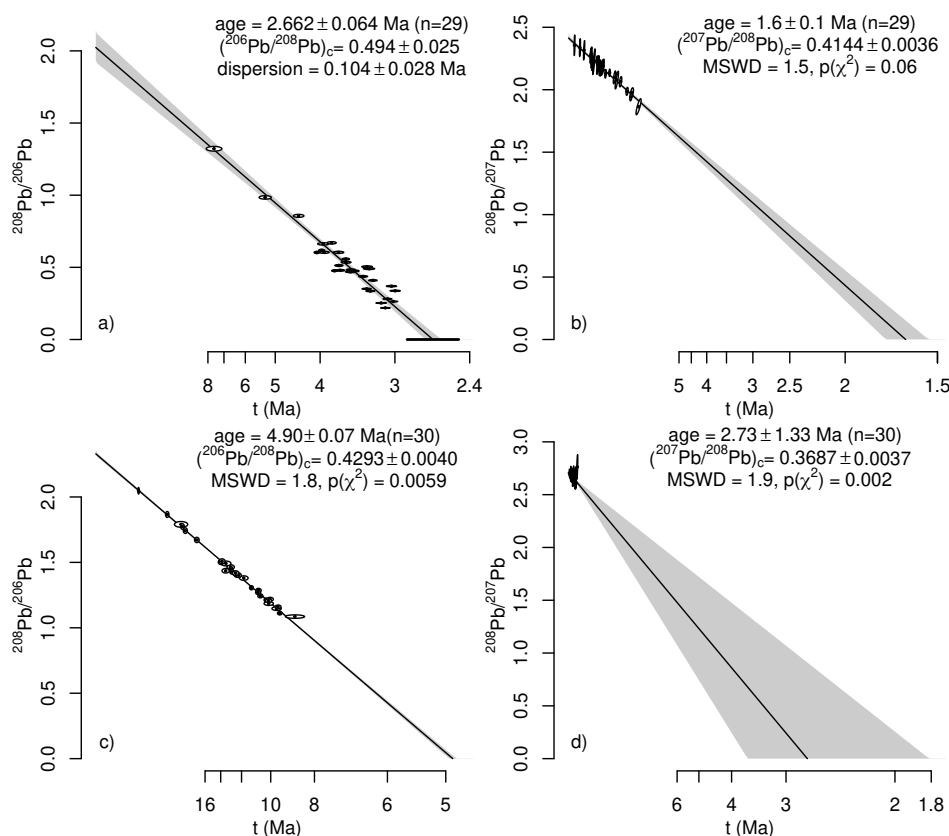
For the final case study, we will return from Israel to the Botovskaya cave deposits in Siberia. Section 7.1 and Figure 7 show abundant evidence that this cave is strongly enriched in initial  $^{234}\text{U}$ , with  $[34/38]_i$ -values ranging from 3 to 5 according to the results of Vaks et al. (2020). The effect of this strong disequilibrium can be confidently undone for the young ( $< 500$  ka) speleothems shown in Figure 7. However, Botovskaya cave also contains speleothems that are considerably older than this, going all the way back to the Plio-Pleistocene. By now it should be clear that the  $^{206}\text{Pb}/^{238}\text{U}$  method is ill suited to unlock this older archive. Figure 9 summarises some preliminary U–Pb results from two of these older cave deposits (sample SB-1625-22 and sample SB-72-8), obtained by LA-ICP-MS.

As mentioned before under the discussion of the Hoogland data, the  $^{204}\text{Pb}$  measurements produced by this technique are imprecise and potentially inaccurate. Fortunately, in this case,  $^{208}\text{Pb}$  was measured and can be used as a substitute for  $^{204}\text{Pb}$ . Th/U ratios (also measured by LA-ICP-MS) were extremely low, allowing us to ignore the radiogenic  $^{208}\text{Pb}$  contribution.



280 The uncorrected  $^{206}\text{Pb}/^{238}\text{U}$  isochron age of sample SB-1625-22 is  $2.66 \pm 0.10$  Ma and exhibits significant overdispersion with respect to the analytical uncertainties (MSWD=36). Model-3 isochron regression (*sensu* Vermeesch, 2024) indicates that this excess scatter is equivalent to an age dispersion of  $104 \pm 28$  kyr (Figure 9a). Given the antiquity of the sample and the difficulty of measuring  $[34/38]_m$  by LA-ICP-MS, no initial disequilibrium measurement was made. Switching from  $^{206}\text{U}/^{238}\text{U}$  to  $^{207}\text{Pb}/^{235}\text{U}$  isochron space lowers the age to  $1.60 \pm 0.10$  Ma whilst reducing the dispersion of the data around the isochron line (MSWD=1.5, Figure 9b). As a ‘sanity check’, to verify the accuracy of this result, it is useful to point out that a  $[34/38]_i$ -value of 3.9 would bring the corrected  $^{206}\text{Pb}/^{238}\text{U}$  isochron in alignment with the  $^{207}\text{Pb}/^{235}\text{U}$  isochron. Such a value is consistent with the initial activity ratios of the more recent Botovskaya deposits (Figure 7b). This not only supports the accuracy of the  $^{207}\text{Pb}/^{235}\text{U}$  isochron results, but also suggests that the  $[34/38]_i$  ratios have remained stable over hundreds of thousands of years.

290 We would like to conclude the results section by drawing attention to the fact that the  $^{207}\text{Pb}/^{235}\text{U}$  method is not always successful. Figures 9c and d show that Botovskaya sample SB-72-8 produces a well defined linear array in  $^{206}\text{Pb}/^{238}\text{U}$  isochron space, but fails to do so in  $^{207}\text{Pb}/^{235}\text{U}$  isochron space. Unfortunately, such cases are not rare. The  $^{207}\text{Pb}/^{235}\text{U}$  approach only works in samples that are sufficiently rich in U and sufficiently poor in common Pb. Speleothems from Botovskaya are rich in U (30–170 ppm for SB-72-8), so that here the problem seems to originate from common Pb (0.4–4 ppm for SB-72-8).



295





**Figure 9.** LA-ICP-MS data for two speleothems from Botovskaya cave in Siberia. a) model-3  $^{206}\text{Pb}/^{238}\text{U}$  isochron regression for sample SB-1625-22. The equivalent model-1 isochron age (with MSWD=9) is  $2.65 \pm 0.10$  Ma. b) model-1  $^{207}\text{Pb}/^{235}\text{U}$  isochron for SB-1625-22; c) model-1  $^{206}\text{Pb}/^{238}\text{U}$  and d)  $^{207}\text{Pb}/^{235}\text{U}$  isochrons for sample SB-72-8 ( $2.73 \pm 1.33$  Ma).

## 8 Implementation in IsoplotR

All the methods described in this paper have been implemented in the IsoplotR toolbox for geochronological data processing (Vermeesch, 2018). The matrix exponential disequilibrium correction method of Section 2 has been part of IsoplotR since version 3.0, whereas the deterministic Bayesian uncertainty estimation routine of Section 4 was introduced in version 5.2. At the time of writing, IsoplotR (version 6.4) supports twelve different U–Pb data formats. Disequilibrium corrected U–Pb isochron regression is available for all these formats, in different forms.

Formats 1–3 contain neither  $^{204}\text{Pb}$  nor  $^{208}\text{Pb}$ . Therefore, isochron regression for these formats must be done by semitotal-Pb/U regression in Tera-Wasserburg concordia space. Formats 4–6 include  $^{204}\text{Pb}$  as a common Pb tracer. These formats permit the calculation of both  $^{206}\text{Pb}/^{238}\text{U}$  and  $^{207}\text{Pb}/^{235}\text{U}$  isochrons, either jointly (by three-dimensional total-Pb/U isochron regression; Ludwig, 1998) or separately. To take full advantage of the  $^{207}\text{Pb}/^{235}\text{U}$  method’s superior accuracy, it is recommended to use the two-dimensional option. Formats 7 and 8 use  $^{208}\text{Pb}$  as a common Pb tracer. They are also amenable to both  $^{206}\text{Pb}/^{238}\text{U}$  and  $^{207}\text{Pb}/^{235}\text{U}$  isochron regression, either jointly (by total Pb/U–Th regression; Vermeesch, 2020) or separately. Formats 9–10 and 11–12 are simplified versions of formats 4–6 and 7–8, respectively, which only permit two-dimensional regression. Formats 9 and 11 are meant for  $^{206}\text{Pb}/^{238}\text{U}$  isochron regression, whereas formats 10 and 12 are meant for  $^{207}\text{Pb}/^{235}\text{U}$  isochron regression.

The disequilibrium corrections can be accessed from IsoplotR’s GUI (either online or offline) by using the ‘isochron’ function and ticking the ‘apply disequilibrium correction’ check box in the options menu. Alternatively, the same functionality can also be accessed from the command-line API. Bayesian uncertainty estimation is possible using either interface, but visualising the posterior distributions of the parameter space is currently only possible from the command line. The following code snippets reproduce some of the key results presented in this paper, using the Hoogland, ASH-15 and Botovskaya datasets. The data can be loaded from .csv files that are provided in the Supplementary Information.

```
library(IsoplotR)
Hoogland <- read.data("Hoogland.csv", method="U-Pb", format=2, ierr=4,
                      d=diseq(U48=list(x=1.00105, sx=0.001, option=2),
                                ThU=list(x=0, sx=0, option=1),
                                PaU=list(x=0, sx=0, option=1)))
ASH15ab <- read.data("ASH15K.csv", method="U-Pb", format=5, ierr=4,
                     d=diseq(U48=list(x=0.99925, sx=0.0015/2, option=2),
                               ThU=list(x=0, sx=0, option=1),
```



```

325         PaU=list (x=0, sx=0, option=1)) )
ASH15cd <- read.data ("ASH15K.csv", method="U-Pb", format=5, ierr=4,
                    d=diseq (ThU=list (x=0, sx=0, option=1) ,
                               PaU=list (x=0, sx=0, option=1)) )
SB1625 <- read.data ("SB-1625-22.csv", method="U-Pb", format=8, ierr=2)
330 SB72 <- read.data ("SB-72-8.csv", method="U-Pb", format=8, ierr=2)
    
```

where `format` specifies one of IsoplotR's aforementioned 12 input formats; `ierr` controls whether the uncertainties are provided at a  $1\sigma$  or  $2\sigma$  confidence level as either absolute values or percentages; and `d` describes the initial disequilibrium conditions. These are a function of four optional arguments named `U48`, `ThU`, `RaU` and `PaU`, corresponding to the  $^{234}\text{U}/^{238}\text{U}$ ,  $^{230}\text{Th}/^{238}\text{U}$ ,  $^{226}\text{Ra}/^{238}\text{U}$  and  $^{231}\text{Pa}/^{235}\text{U}$  activity ratios, respectively. Each of these values and their uncertainties can either be

335 specified as initial ratios (`option=1`) or as measured ratios (`option=2`). Omitting an argument or assigning `option=0` enforces secular equilibrium. Figures 2a, 8a–b and 9 were generated using IsoplotR's `isochron` function:

```

isochron (Hoogland) # 2a
isochron (ASH15cd, joint=FALSE, type=1, taxis=TRUE) # 8c
isochron (ASH15cd, joint=FALSE, type=2, taxis=TRUE) # 8d
340 isochron (SB1625, model=3, joint=FALSE, type=1, taxis=TRUE) # 9a
isochron (SB1625, joint=FALSE, type=2, taxis=TRUE) # 9b
isochron (SB72, joint=FALSE, type=1, taxis=TRUE) # 9c
isochron (SB72, joint=FALSE, type=2, taxis=TRUE) # 9d
    
```

where `joint=FALSE` decouples the  $^{206}\text{Pb}/^{238}\text{U}$  and  $^{207}\text{Pb}/^{235}\text{U}$  methods to produce 2D isochrons; `type=1` produces

345  $^{206}\text{Pb}/^{238}\text{U}$  isochrons and `type=2`  $^{207}\text{Pb}/^{235}\text{U}$  isochrons; `taxis` labels the horizontal axis with units of geologic time; and `model=3` estimates the age dispersion (Vermeesch, 2024). For the Hoogland and ASH-15 data, the `isochron` function automatically carries out the Bayesian uncertainty estimation. This calculation is done in the background by the `ludwig` function, which includes an option to visualise the posterior distributions of the initial  $^{234}\text{U}/^{238}\text{U}$  activity ratios and isochron ages:

```

ludwig (Hoogland, type=1, plot=TRUE) # 5b and 5c
350 ludwig (ASH15ab, type=1, plot=TRUE) # 8a and 8b
    
```

## 9 Conclusions

In this paper, we presented a critical appraisal of carbonate U–Pb geochronology, and proposed three improvements to the technique. First, we introduced a matrix exponential solution to the initial disequilibrium problem. This solution produces identical results to the conventional solution by Engel et al. (2019), but can be written out more succinctly. Second, we presented

355 a deterministic Bayesian algorithm to quantify the statistical uncertainty associated with the disequilibrium correction. This



algorithm was used to demonstrate that, for samples older than 2 Ma, disequilibrium-corrected  $^{206}\text{Pb}/^{238}\text{U}$  geochronology is unreliable. Third, we advocated the use of the  $^{207}\text{Pb}/^{235}\text{U}$  isochron method as a more accurate alternative to the  $^{206}\text{Pb}/^{238}\text{U}$  method.

Although our findings are most relevant to young carbonates, the inaccuracy of the  $^{206}\text{Pb}/^{238}\text{U}$  method equally applies  
360 to old samples. Only the relative difference between the  $^{206}\text{Pb}/^{238}\text{U}$  and  $^{207}\text{Pb}/^{235}\text{U}$  ages reduces with time. The absolute difference remains the same, as the following example shows. Consider four cogenetic carbonate samples that contain no initial Th or Pa, and are characterised by  $[34/38]_i$ -values of 0, 2, 4 and 8, respectively. Once this initial disequilibrium has decayed away (after 2 Ma), an absolute age difference between the uncorrected  $^{206}\text{Pb}/^{238}\text{U}$  and  $^{207}\text{Pb}/^{235}\text{U}$  clocks of  $-0.4$ ,  $+0.3$ ,  $+1.0$  and  $+2.4$  Ma remains. The corresponding systematic uncertainty cannot be removed without making unverifiable  
365 assumptions about the initial  $^{234}\text{U}/^{238}\text{U}$  activity ratio. For samples older than  $> 100$  Ma, say, the systematic error caused by initial disequilibrium is generally smaller than the random errors associated with the isotope ratio measurements. However, given a sufficiently precise set of isochrons, it is theoretically possible to reconstruct the U-disequilibrium conditions at the time of isotopic closure from the difference between the  $^{206}\text{Pb}/^{238}\text{U}$  and  $^{207}\text{Pb}/^{235}\text{U}$  clocks.

Engel et al. (2019) advocate using the same procedure in Quaternary studies. They propose a two-step procedure, whereby  
370 the difference between the  $^{206}\text{Pb}/^{238}\text{U}$  and  $^{207}\text{Pb}/^{235}\text{U}$  dates is used to estimate  $[34/38]_i$ ; and this  $[34/38]_i$ -value is then used to calculate a corrected  $^{206}\text{Pb}/^{238}\text{U}$ -age. *IsoplotR* implements a one-step algorithm that achieves the same goal using the total-Pb/U algorithm of Ludwig (1998) and the total-Pb/U–Th algorithm of Vermeesch (2020). However, we would like to add a note of caution about the usefulness of this joint regression procedure. Beyond 2 Ma, all the age-resolving power of the paired  $^{206}\text{Pb}/^{238}\text{U}$  and  $^{207}\text{Pb}/^{235}\text{U}$  approach resides in the  $^{207}\text{Pb}/^{235}\text{U}$  clock, so the  $^{206}\text{Pb}/^{238}\text{U}$  data add no value (Vermeesch et al.,  
375 2025. A preprint of this accepted manuscript can be downloaded from <https://tinyurl.com/Taung2025>).

*Code and data availability.* *IsoplotR* is free software released under the GPL-3 license. The package and its source code are available from <https://cran.r-project.org/package=IsoplotR> (last access: December 14, 2024, Vermeesch, 2018). The test data used in Section 8 are provided in the supplementary information at <https://github.com/pvermeesch/supplements>.

*Author contributions.* NM developed the matrix exponential solution to the initial disequilibrium problem (McLean et al., 2016); PV devel-  
380 oped the deterministic Bayesian inversion algorithm; RP proposed the  $^{207}\text{Pb}/^{235}\text{U}$  fix to the  $^{206}\text{Pb}/^{238}\text{U}$  problems; AV, TG and SB provided the Siberian data; PV wrote the paper, with feedback from the other authors.

*Competing interests.* PV and NM are Associate Editors of *Geochronology*.



*Acknowledgements.* This research has been supported by the Natural Environment Research Council (grant no. NE/T001518/1, awarded to PV) and the Leverhulme Trust (grant no. RPG-20202-334, awarded to SFMB).



## 385 References

- Cheng, H., Edwards, R. L., Shen, C.-C., Polyak, V. J., Asmerom, Y., Woodhead, J., Hellstrom, J., Wang, Y., Kong, X., Spötl, C., et al.: Improvements in  $^{230}\text{Th}$  dating,  $^{230}\text{Th}$  and  $^{234}\text{U}$  half-life values, and U–Th isotopic measurements by multi-collector inductively coupled plasma mass spectrometry, *Earth and Planetary Science Letters*, 371, 82–91, 2013.
- Engel, J., Woodhead, J., Hellstrom, J., Maas, R., Drysdale, R., and Ford, D.: Corrections for initial isotopic disequilibrium in the speleothem U–Pb dating method, *Quaternary Geochronology*, 54, 101 009, 2019.
- Fleischer, R. L.: Alpha-recoil damage and solution effects in minerals: uranium isotopic disequilibrium and radon release, *Geochimica et Cosmochimica Acta*, 46, 2191–2201, 1982.
- Kaufman, A. and Broecker, W.: Comparison of  $\text{Th}^{230}$  and  $\text{C}^{14}$  ages for carbonate materials from Lakes Lahontan and Bonneville, *Journal of Geophysical Research*, 70, 4039–4054, 1965.
- 395 Kronfeld, J., Vogel, J., and Talma, A.: A new explanation for extreme  $^{234}\text{U}/^{238}\text{U}$  disequilibria in a dolomitic aquifer, *Earth and Planetary Science Letters*, 123, 81–93, 1994.
- Ludwig, K. R.: On the treatment of concordant uranium-lead ages, *Geochimica et Cosmochimica Acta*, 62, 665–676, [https://doi.org/10.1016/S0016-7037\(98\)00059-3](https://doi.org/10.1016/S0016-7037(98)00059-3), 1998.
- Ludwig, K. R.: User’s manual for Isoplot 3.00: a geochronological toolkit for Microsoft Excel, Berkeley Geochronology Center Special Publication, 4, 2003a.
- 400 Ludwig, K. R.: Mathematical–statistical treatment of data and errors for  $^{230}\text{Th}/\text{U}$  geochronology, *Reviews in Mineralogy and Geochemistry*, 52, 631–656, 2003b.
- Mason, A. J., Henderson, G. M., and Vaks, A.: An acetic acid-based extraction protocol for the recovery of U, Th and Pb from calcium carbonates for U–(Th)–Pb geochronology, *Geostandards and Geoanalytical Research*, 37, 261–275, 2013.
- 405 McLean, N. M., Smith, C. J. M., Roberts, N. M. W., and Richards, D. A.: Connecting the U–Th and U–Pb Chronometers: New Algorithms and Applications, AGU Fall Meeting Abstracts, 2016.
- Nuriel, P., Wotzlaw, J.-F., Ovtcharova, M., Vaks, A., Stremtan, C., Šála, M., Roberts, N. M. W., and Kylander-Clark, A. R. C.: The use of ASH-15 flowstone as a matrix-matched reference material for laser-ablation U–Pb geochronology of calcite, *Geochronology*, 3, 35–47, <https://doi.org/10.5194/gchron-3-35-2021>, 2021.
- 410 Pickering, R., Herries, A. I., Woodhead, J. D., Hellstrom, J. C., Green, H. E., Paul, B., Ritzman, T., Strait, D. S., Schoville, B. J., and Hancox, P. J.: U–Pb-dated flowstones restrict South African early hominin record to dry climate phases, *Nature*, 565, 226, 2019.
- Pollard, T., Woodhead, J., Hellstrom, J., Engel, J., Powell, R., and Drysdale, R.: DQPB: software for calculating disequilibrium U–Pb ages, *Geochronology*, 5, 181–196, 2023.
- Porcelli, D. and Swarzenski, P. W.: The behavior of U-and Th-series nuclides in groundwater, *Reviews in mineralogy and geochemistry*, 52, 317–361, 2003.
- 415 Richards, D. A., Bottrell, S. H., Cliff, R. A., Ströhle, K., and Rowe, P. J.: U–Pb dating of a speleothem of Quaternary age, *Geochimica et Cosmochimica Acta*, 62, 3683–3688, 1998.
- Roberts, N. M., Drost, K., Horstwood, M. S., Condon, D. J., Chew, D., Drake, H., Milodowski, A. E., McLean, N. M., Smye, A. J., Walker, R. J., et al.: Laser ablation inductively coupled plasma mass spectrometry (LA-ICP-MS) U–Pb carbonate geochronology: strategies, progress, and limitations, *Geochronology*, 2, 33–61, 2020.
- 420



- Schärer, U.: The effect of initial  $^{230}\text{Th}$  disequilibrium on young UPb ages: the Makalu case, Himalaya, Earth and Planetary Science Letters, 67, 191–204, 1984.
- Vaks, A., Bar-Matthews, M., Matthews, A., Ayalon, A., and Frumkin, A.: Middle-Late Quaternary paleoclimate of northern margins of the Saharan-Arabian Desert: reconstruction from speleothems of Negev Desert, Israel, Quaternary Science Reviews, 29, 2647–2662, 2010.
- 425 Vaks, A., Gutareva, O. S., Breitenbach, S. F., Avirmed, E., Mason, A. J., Thomas, A. L., Osinzev, A. V., Kononov, A. M., and Henderson, G. M.: Speleothems reveal 500,000-year history of Siberian permafrost, Science, 340, 183–186, 2013a.
- Vaks, A., Woodhead, J., Bar-Matthews, M., Ayalon, A., Cliff, R., Zilberman, T., Matthews, A., and Frumkin, A.: Pliocene–Pleistocene climate of the northern margin of Saharan–Arabian Desert recorded in speleothems from the Negev Desert, Israel, Earth and Planetary Science Letters, 368, 88–100, 2013b.
- 430 Vaks, A., Mason, A., Breitenbach, S., Kononov, A., Osinzev, A., Rosenshaft, M., Borshevsky, A., Gutareva, O., and Henderson, G.: Palaeoclimate evidence of vulnerable permafrost during times of low sea ice, Nature, 577, 221–225, 2020.
- Vermeesch, P.: IsoplotR: a free and open toolbox for geochronology, Geoscience Frontiers, 9, 1479–1493, 2018.
- Vermeesch, P.: Unifying the U–Pb and Th–Pb methods: joint isochron regression and common Pb correction, Geochronology, 2, 119–131, 2020.
- 435 Vermeesch, P.: Errorchrons and anchored isochrons in IsoplotR, Geochronology, 2024, 2024.
- Vermeesch, P., Hopley, P., Roberts, N., and Parrish, R.: Geochronology of Taung and other southern African australopiths, in: One hundred years of *Australopithecus africanus*, edited by Wood, B. A., Grine, F. E., and Smith, H. B., chap. 4, 2025. A preprint of this accepted manuscript can be downloaded from <https://tinyurl.com/Taung2025>.
- Woodhead, J., Hellstrom, J., Maas, R., Drysdale, R., Zanchetta, G., Devine, P., and Taylor, E.: U–Pb geochronology of speleothems by  
 440 MC-ICPMS, Quaternary Geochronology, 1, 208–221, 2006.